DALTON
FULL PAPER

Synthesis of a sulfido-capped triiron cluster with bridging phosphido ligands and its reactions with alkynes, phosphites and phosphines †

Nick Choi,[a] Gráinne Conole,[a] Margalith Kessler,[a] Jason D. King,[b]*‡ Martin J. Mays,[b]* Mary McPartlin,[a] Giles E. Pateman[b] and Gregory A. Solan[c]*

[a] *School of Applied Chemistry, University of North London, Holloway Road, London, UK N7 8DB*
[b] *Department of Chemistry, Lensfield Road, Cambridge, UK CB2 1EW*
[c] *Department of Chemistry, University of Leicester, University Road, Leicester, UK LE1 7RH*

Received 22nd July 1999, Accepted 4th October 1999

Treatment of $[Fe(CO)_5]$ with $Ph_2P(SCMe_3)$ at elevated temperature and pressure afforded, as the major product, the sulfur-capped trinuclear iron cluster $[Fe_3(\mu_3\text{-}S)(\mu\text{-}PPh_2)_2(\mu\text{-}CO)(CO)_6]$ **1**, in which two Fe–Fe edges are bridged by phosphido groups and the other by a carbonyl group. Also isolated in low yield from this reaction was the tetranuclear iron complex $[\{Fe_2(\mu\text{-}PPh_2)(CO)_6\}_2(\mu_4\text{-}S_2)]$ **2**, which comprises two phosphido-sulfido-bridged diiron fragments linked by an S–S bond. In contrast it has been demonstrated that the reaction of $[Fe(CO)_5]$ with $Ph_2P(SPh)$ gives the discrete dinuclear complex $[Fe_2(\mu\text{-}PPh_2)(\mu\text{-}SPh)(CO)_6]$ in which a sulfur–carbon bond has been retained. The reaction of **1** with organo-phosphites and -phosphines results in preservation of the triiron core and monosubstitution of a carbonyl group to give $[Fe_3(\mu_3\text{-}S)(\mu\text{-}PPh_2)_2(\mu\text{-}CO)(CO)_5(L)]$ [L = $P(OMe)_3$ **3a**, $P(OPh)_3$ **3b**, $PPhMe_2$ **3c** or PPh_3 **3d**]. On reaction of **1** with terminal alkynes, RC≡CH [R = Ph or CH_2OH], degradation of the trinuclear framework results to give the metallacyclic-bridged bimetallic complexes $[Fe_2(\mu\text{-}PPh_2CHCRS)(\mu\text{-}PPh_2CHCR)(CO)_4]$ [R = Ph **4a** or CH_2OH **4b**] in which new sulfur–carbon and phosphorus–carbon bonds have formed. In addition, the phosphido-bridged species $[Fe_2(\mu\text{-}PPh_2)(\mu\text{-}PPh_2CHCPhS)(CO)_5]$ **5** is isolated as a minor product from the reaction of **1** with PhC≡CH. The structures of complexes **1**, **2**, **3c** and **4a** have been determined by single crystal X-ray diffraction analysis and pathways are postulated for the formation of the various products.

Introduction

Interest in multinuclear transition metal complexes incorporating sulfur atoms has been widespread for a variety of reasons including the range of structural types,[1] their connection with biological processes[2] and their relevance to the hydrodesulfurisation process.[3] In addition a number of complexes of the type $M_3(\mu_3\text{-}S)$ (M = transition metal) have been used as efficient catalysts in the cyclotrimerisation of terminal alkynes to give benzene derivatives.[4] The trinuclear species remains intact during the cyclotrimerisation process, presumably due at least in part to the stabilising effect of the sulfur cap. In a similar way the phosphido group ($\mu\text{-}PR_2$) has often been used as an inert bridging ligand capable of preventing fragmentation of a polynuclear catalyst during a given organic transformation,[5] although there is a growing list of examples in which the $\mu\text{-}PR_2$ group itself can participate in the transformation.[6]

We have been interested in harnessing the potential stability introduced by having both a capping sulfur atom and bridging phosphido groups within the same polynuclear framework. In particular, we have found that the thiophosphine ligand, $Ph_2P(SPh)$, acts as a convenient source of phosphide and sulfide/thiolate fragments on treatment with a metal carbonyl complex, the precise nature of the sulfur-containing fragment being dependent on the metal carbonyl complex employed.[7–9] For example, the reaction of cobalt carbonyl with $Ph_2P(SPh)$ gives a range of sulfur-capped tricobalt complexes $[Co_3(\mu_3\text{-}S)(\mu\text{-}PPh_2)(CO)_{7-x}(PPh_3)_x]$ ($x = 0$, 1 or 2) in each of which one edge of the metal triangle is bridged by a PPh_2 group.[7] In contrast, treatment of iron carbonyl with $Ph_2P(SPh)$ results in a dinuclear complex, $[Fe_2(\mu\text{-}PPh_2)(\mu\text{-}SPh)(CO)_6]$, in which the S–C bond is retained within the SPh group.[10] The apparent subtle factors that influence whether S–C bond scission occurs within the generated SPh fragment have prompted us to prepare new $Ph_2P(SR)$ (R = alkyl) ligands and examine their reactions with metal carbonyl complexes.[11]

In this report we describe the synthesis of the sulfur-capped triiron complex $[Fe_3(\mu_3\text{-}S)(\mu\text{-}PPh_2)_2(\mu\text{-}CO)(CO)_6]$ **1** from the reaction of iron carbonyl with $Ph_2P(SCMe_3)$ and examine the reactions of **1** with triorgano-phosphites, -phosphines and terminal alkynes.

Results and discussion

I. Reaction of $[Fe(CO)_5]$ with $Ph_2P(SCMe_3)$ at elevated temperature and pressure

The reaction of $[Fe(CO)_5]$ with $Ph_2P(SCMe_3)$ in toluene at 423 K and 5 atm CO gives $[Fe_3(\mu_3\text{-}S)(\mu\text{-}PPh_2)_2(\mu\text{-}CO)(CO)_6]$ **1** as the major product along with $[\{Fe_2(\mu\text{-}PPh_2)(CO)_6\}_2(\mu_4\text{-}S_2)]$ **2** (see Scheme 1). Both complexes have been characterised by ^1H, ^{13}C, ^{31}P NMR and IR spectroscopy and by mass spectrometry and microanalysis (see Table 1 and Experimental section). In addition **1** and **2** have been the subjects of single crystal X-ray diffraction studies. A partial determination of the molecular structure of complex **1** was made; this is depicted in Fig. 1. The X-ray analysis is consistent with the proposed structure[12] but the poor quality of the data precludes discussion of the structural details.

The spectroscopic properties of complex **1** are consistent with the solid-state structure being maintained in solution. The

† *Supplementary data available*: rotatable 3-D crystal structure diagram in CHIME format. See http://www.rsc.org/suppdata/dt/1999/3941/
‡ *Present address*: Department of Chemistry, University of Montana, Missoula 59812, Montana, USA.

Table 1 Infrared, ^{1}H and ^{31}P NMR data for complexes **1**–**5**

Compound	$\tilde{\nu}$(CO)[a]/cm^{-1}	^{1}H NMR (δ)[b]	^{31}P NMR (δ)[c]
1	2042m, 2004s, 1980s, 1875m	7.9–6.9[m, 20 H, Ph]	149.9[s, μ-PPh_2]
2	2060m, 2020vs, 1998s, 1979m, 1966(sh)	7.9–7.0[m, 20 H, Ph]	69.1[s, μ-PPh_2]
3a	2014s, 1984vs, 1958vs, 1839m	7.9–6.9[m, 25 H, Ph], 3.31[d, ^3J(PH) 11.1, 9 H, $P(OMe)_3$]	148.8[d, ^2J(PP) 48, μ-PPh_2], 133.0[dd, ^2J(PP) 55, μ-PPh_2], 6.3[d, ^2J(PP) 60, $P(OMe)_3$]
3b	2022s, 1994s, 1972m, 1855m	7.8–6.9[m, 35 H, Ph]	148.6[d, ^2J(PP) 52, μ-PPh_2], 132.9[dd, ^2J(PP) 57, 57, μ-PPh_2], 23.2[d, ^2J(PP) 64, $P(OPh)_3$]
3c	2015s, 1986s, 1962m, 1837m	7.9–7.0[m, 25 H, Ph], 1.51[s, br, $PPhMe_2$]	151.2[s, br, μ-PPh_2], 116.9[s, br, μ-PPh_2], −114.8[d, ^2J(PP) 24.4, PMe_2Ph]
3d	2021s, 1990vs, 1975vs, 1954w, 1853m	7.8–6.9[m, 35 H, Ph]	148.8[d, ^2J(PP) 60.0, μ-PPh_2], 112.5[dd, ^2J(PP) 32.2, 60.0, μ-PPh_2], −78.0[d, ^2J(PP) 30.5, PPh_3]
4a	2008s, 1979s, 1953m, 1937m	8.0–6.9[m, 30 H, Ph], 6.39[dd, ^2J(PH) 20.4, ^4J(PH) 5.8, 1 H, PPh_2-C*H*CPh], 4.08[s, 1 H, PPh_2C*H*-CPhS]	−66.2[d, ^3J(PP) 18.3], −68.2[d, ^3J(PP) 18.3] corresponding to [μ-PPh_2CHCPhS] and [μ-PPh_2CHCPh]
4b	2002s, 1968s, 1942m, 1923m	8.0–6.9[m, 20 H, Ph], 6.40[dd, ^2J(PH) 20.3, ^4J(PH) 6.6, 1 H, PPh_2C*H*(CH_2OH)], 4.84[m, 2 H, CH(C*H*$_2$OH)], 4.65[m, 2 H, CH-(C*H*$_2$OH)], 3.67[d, ^2J(PH) 1.8, 1 H, PPh_2C*H*(CH_2OH)], 2.79[s, br, 1 H, CH_2O*H*], 2.00[s, br, 1 H, CH_2O*H*]	−66.8[d, ^3J(PP) 18.3], −68.3[d, ^3J(PP) 18.3], corresponding to [μ-PPh_2CHC(CH_2OH)S] and [μ-PPh_2CHC(CH_2OH)]
5	2031s, 1983s, 1955m, 1928m	8.0–7.0[m, 25 H, Ph], 6.88[d, ^2J(PH) 6.8, 1 H, PPh_2C*H*CPhS]	−1.5[d, ^2J(PP) 78, μ-PPh_2], −54.2[d, ^2J(PP) 78, μ-PPh_2-CHCPhS]

[a] Recorded in *n*-hexane solution. [b] ^{1}H chemical shifts (δ) in ppm relative to $SiMe_4$ (0.0 ppm), coupling constants in Hz in $CDCl_3$ at 293 K. [c] ^{31}P chemical shifts (δ) in ppm relative to external $P(OMe)_3$ (0.0 ppm) (upfield shifts negative), {^{1}H}-gated decoupled, measured in $CDCl_3$ at 293 K. To reference relative to 85% H_3PO_4 add 140.2 to tabulated values.

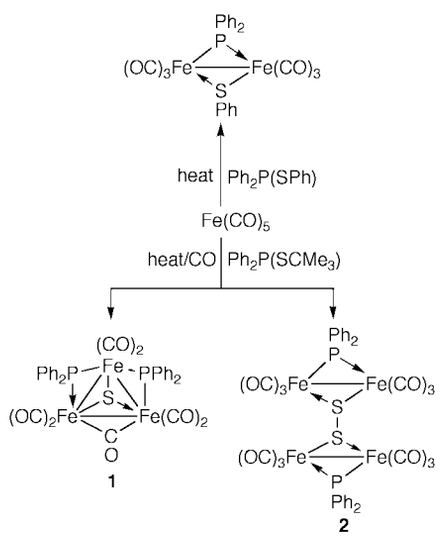

Scheme 1 Products from the reactions of $[Fe(CO)_5]$ with either $Ph_2P(SCMe_3)$ or $Ph_2P(SPh)$.[10]

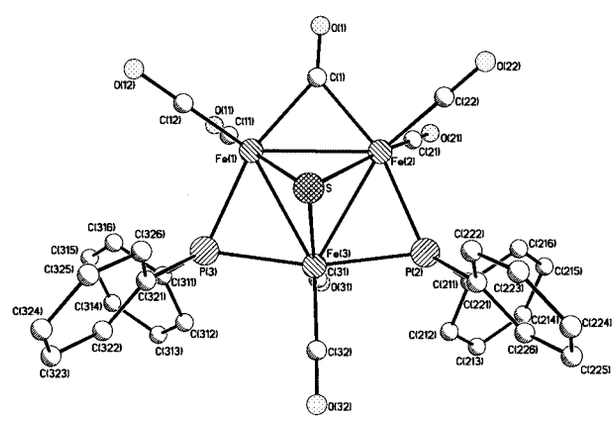

Fig. 1 Partially determined molecular structure of $[Fe_3(\mu_3\text{-}S)(\mu\text{-}PPh_2)_2(\mu\text{-}CO)(CO)_6]$ **1** including the atom numbering scheme. Hydrogen atoms have been omitted for clarity.

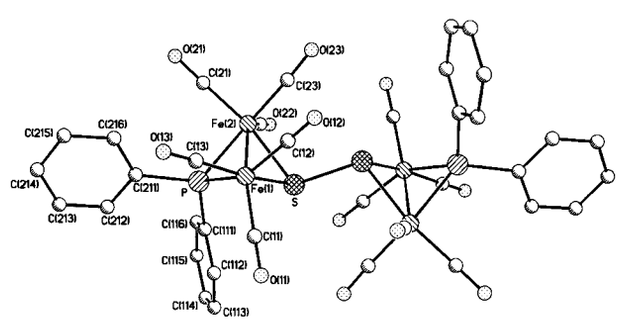

Fig. 2 Molecular structure of the complex $[\{Fe_2(\mu\text{-}PPh_2)(CO)_6\}_2(\mu\text{-}S_2)]$ **2** including the atom numbering scheme. Hydrogen atoms have been omitted for clarity. An inversion centre exists at the midpoint of the disulfide bond.

IR spectrum shows, in addition to three terminal ν_{CO} bands, an absorption at lower wavenumber [1875 cm^{-1}] indicating the presence of a bridging carbonyl group. The ^{31}P-{^{1}H} NMR spectrum [relative to $P(OMe)_3$ (δ 0.0)] of this complex displays one singlet resonance corresponding to the equivalent bridging phosphorus groups [δ 149.9] while the ^{13}C-{^{1}H} NMR spectrum shows, in addition to phenyl resonances, two doublet of doublet carbonyl resonances [δ 214.6{^2J(PC) 16, ^2J(P′C) 16} and 208.8{^2J(PC) 12, ^2J(P′C) 12 Hz}] implying localised fluxionality at room temperature on the NMR timescale. It is possible that the five carbonyl ligands residing on the iron atoms of the iron–iron edge, which is not bridged by a phosphido group, may fluxionate to give one resonance with the other signal being due to the equivalent carbonyl ligands on the remaining iron atom.

The molecular structure of complex **2**, which has a crystallographic inversion at the midpoint of the disulfide bond, is illustrated in Fig. 2; Table 2 lists selected bond distances and angles. The two symmetry-related pairs of iron atoms are each

Table 2 Selected bond distances (Å) and angles (°) for complex $[\{Fe_2(\mu\text{-}PPh_2)(CO)_6\}_2(\mu_4\text{-}S_2)]$ **2**

Fe(1)–Fe(2)	2.614(1)	Fe(1)–S	2.253(1)
Fe(1)–P	2.242(2)	Fe(2)–S	2.261(1)
Fe(2)–P	2.238(1)	P–C(111)	1.827(3)
P–C(211)	1.834(3)	S–S′	2.130(2)
Fe–C (carbonyl)	1.781(4)–1.810(4)	C–O (carbonyl)	1.134(5)–1.145(4)
Fe(2)–Fe(1)–P	54.23(4)	Fe(2)–Fe(1)–S	54.75(4)
Fe(2)–Fe(1)–C(11)	147.2(1)	Fe(2)–Fe(1)–C(12)	97.6(2)
Fe(2)–Fe(1)–C(13)	112.8(1)	P–Fe(1)–S	76.35(5)
P–Fe(1)–C(11)	108.9(1)	P–Fe(1)–C(12)	150.3(2)
P–Fe(1)–C(13)	92.9(1)	S–Fe(1)–C(11)	96.1(1)
S–Fe(1)–C(12)	95.4(1)	S–Fe(1)–C(13)	166.9(1)
C(11)–Fe(1)–C(12)	100.3(2)	C(11)–Fe(1)–C(13)	94.5(2)
C(12)–Fe(1)–C(13)	90.3(2)	Fe(1)–Fe(2)–P	54.36(4)
Fe(1)–Fe(2)–S	54.46(3)	Fe(1)–Fe(2)–C(21)	113.2(2)
Fe(1)–Fe(2)–C(22)	144.9(2)	Fe(1)–Fe(2)–C(23)	97.7(2)
P–Fe(2)–S	76.26(4)	P–Fe(2)–C(21)	92.1(1)
P–Fe(2)–C(22)	108.1(1)	P–Fe(2)–C(23)	150.4(2)
S–Fe(2)–C(21)	166.5(1)	S–Fe(2)–C(22)	93.9(2)
S–Fe(2)–C(23)	96.1(1)	C(21)–Fe(2)–C(22)	96.2(2)
C(21)–Fe(2)–C(23)	90.7(2)	C(22)–Fe(2)–C(23)	100.9(2)
Fe(1)–P–Fe(2)	71.41(4)	C(111)–P–C(211)	102.0(1)
Fe(1)–S–Fe(2)	70.79(4)	Fe(1)–S–S′	109.85(7)
Fe(2)–S–S′	109.88(6)		

bridged by a phosphido group (μ-PPh_2) and a sulfur atom (μ-S). Both Fe(1) and Fe(2) are additionally ligated by three terminal carbonyl groups (one axial and two equatorial), completing a distorted octahedral arrangement around each metal centre. Each of the centrosymmetrically related $[Fe_2(\mu\text{-}P)(\mu\text{-}S)]$ cores displays a 'butterfly' arrangement with a dihedral angle of 82.1° between the Fe_2P and Fe_2S planes. The Fe(1)–Fe(2) distance [2.614(1) Å] is identical to that in the diiron complex $[Fe_2(\mu\text{-}PPh_2)(\mu\text{-}SPh)(CO)_6]$ [2.614(3) Å],[10] which also possesses such a Fe_2PS 'butterfly' core. The only significant difference between the co-ordination of the Fe atoms in the latter structure and in **2** concerns the Fe–S bond lengths (0.03 Å longer in $[Fe_2(\mu\text{-}PPh_2)(\mu\text{-}SPh)(CO)_6]$ than in **2**). The two $[Fe_2(\mu\text{-}PPh_2)(\mu\text{-}S)(CO)_6]$ units in **2** are coupled by a S–S bond [S–S′ 2.130(2) Å]. It is of note that **2** is thus a rare example of a complex containing a μ_4-S_2 ligand.[13] The bridging Fe_2–S–S–Fe_2 structural unit is also found in the tetranuclear anion[14] $[\{Fe_2(\mu\text{-}S)(CO)_6\}_2(\mu\text{-}S_2)]^{2-}$, which has a longer Fe–Fe bond [2.614(1) **2** *vs.* 2.518(1) Å] but a shorter S–S bond [2.130(2) **2** *vs.* 2.164(2) Å] than **2**.

The IR spectrum of complex **2** is similar to that of $[Fe_2(\mu\text{-}PPh_2)(\mu\text{-}SPh)(CO)_6]$[10] with four absorptions in the terminal carbonyl region. The $^{31}P\text{-}\{^1H\}$ NMR spectrum displays one sharp resonance in the range typical for bridging phosphido groups [δ 69.1][5] while the FAB mass spectrum shows a molecular ion peak along with fragmentation peaks corresponding to the loss of up to six carbonyl groups.

It is noteworthy that the reaction of $[Fe(CO)_5]$ with Ph_2P(SPh) yields as the sole product the complex $[Fe_2(\mu\text{-}PPh_2)(\mu\text{-}SPh)(CO)_6]$ in which the sulfur–carbon bond has been retained (see Scheme 1). However, the analogous reaction with $Ph_2P(SCMe_3)$ results in S–C bond cleavage in addition to scission of the S–P bond to give either **1** or **2**. The β elimination of butene from similar complexes containing butyl moieties to leave less strongly bonding hydride ligands is widely documented.[15] The elimination of isobutene would lead to the formation of $[Fe_2(\mu\text{-}PPh_2)(\mu\text{-}SH)(CO)_6]$ in which the weak S–H bond could then easily be cleaved to yield **2** *via* dimerisation or could react with a further iron carbonyl species to give **1** (Scheme 2). Similar reactivity has been observed in related isolable SH-bridged complexes to give products resulting from cluster build-up.[16] The ligand Ph_2P(SPh) is apparently not able to undergo such a transformation and the S–C bond is retained under similar conditions.

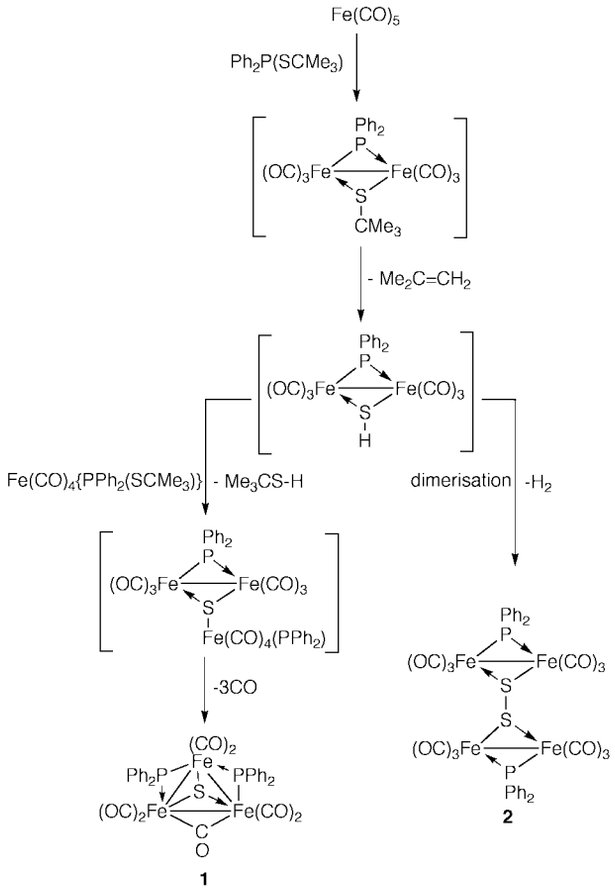

Scheme 2 Proposed pathway for the formation of complexes **1** and **2**.

II. Reaction of $[Fe_3(\mu_3\text{-}S)(\mu\text{-}PPh_2)_2(\mu\text{-}CO)(CO)_6]$ 1 with L at elevated temperature

The reaction of $[Fe_3(\mu_3\text{-}S)(\mu\text{-}PPh_2)_2(\mu\text{-}CO)(CO)_6]$ **1** with L [$P(OMe)_3$, $P(OPh)_3$, $PPhMe_2$ or PPh_3] in toluene at 373 K affords the complexes $[Fe_3(\mu_3\text{-}S)(\mu\text{-}PPh_2)_2(\mu\text{-}CO)(CO)_5(L)]$ [L = $P(OMe)_3$ **3a**, $P(OPh)_3$ **3b**, $PPhMe_2$ **3c** or PPh_3 **3d**] in high yield (see Scheme 3). All the complexes have been characterised by ^1H, ^{13}C, ^{31}P NMR and IR spectroscopy and by mass spectrometry and microanalysis (see Table 1 and Experimental section). In addition **3c** has been the subject of a single crystal X-ray diffraction study.

The molecular structure of $[Fe_3(\mu_3\text{-}S)(\mu\text{-}PPh_2)_2(\mu\text{-}CO)(CO)_5(PPhMe_2)]$ **3c** is shown in Fig. 3 and selected bond distances and angles are listed in Table 3. The structure is essentially the same as that for complex **1** with a sulfur atom capping the triiron base and the three metal–metal edges bridged by phosphido [Fe(1)–Fe(3), Fe(2)–Fe(3)] and carbonyl groups [Fe(1)–Fe(2)]. The structure differs from that in **1** in that a pseudo-equatorial terminal carbonyl group on one of the iron atoms that is attached to both a bridging phosphido and a bridging carbonyl group is replaced by a $PPhMe_2$ ligand.

Attack of $PPhMe_2$ on complex **1** is notably regiospecific in that, as indicated above, the phosphine prefers to adopt a pseudo-equatorial site on an iron atom that is co-ordinated by both the bridging carbonyl and a phosphido group. The symmetry of **1** means that although $PPhMe_2$ may attack at Fe(1) to yield the enantiomer of **3c** depicted in Fig. 3 and discussed above, substitution of the equatorial carbonyl at Fe(2) is equally probable. It must be assumed that reaction of **1** with $PPhMe_2$ results in a racemic mixture, which is spontaneously resolved on crystallisation in the chiral space group $P2_12_12_1$.

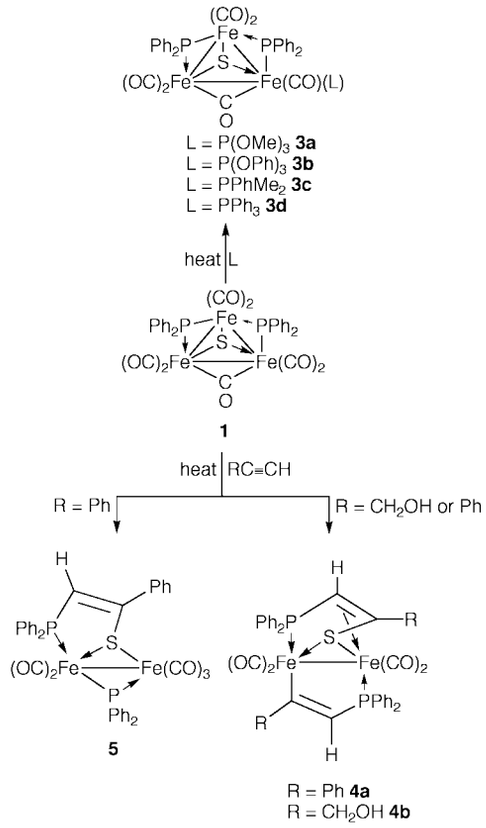

Scheme 3 Products from the reactions of $[Fe_3(\mu_3\text{-}S)(\mu\text{-}PPh_2)_2(\mu\text{-}CO)(CO)_6]$ **1** with alkynes, phosphites and phosphines.

The spectroscopic properties of complex **3c** are consistent with the solid state structure being maintained in solution. On the basis of the close similarity in the spectroscopic data of **3c** with those of **3a**, **3b** and **3d**, analogous structures are ascribed to the latter three complexes. In the IR spectra of **3** the bridging carbonyl groups are seen clearly at lower wavenumbers [1837–1855 cm^{-1}] than the terminal carbonyl groups while molecular ion peaks are observed in the FAB mass spectra of each species. In the $^{31}P\text{-}\{^1H\}$ NMR spectra three resonances are observed correponding to three inequivalent phosphorus environments with the terminal phosphine/phosphite and the remote phosphido group signals taking the form of doublets while the phosphido group adjacent to both gives rise to a doublet of doublets. The $^{13}C\text{-}\{^1H\}$ NMR spectra show, in addition to phenyl and phosphine ligand resonances, two double doublet carbonyl signals at *ca.* δ 216 and *ca.* 210. This implies that some localised fluxionality of the carbonyl groups within the complexes occurs at room temperature on the NMR timescale. It is possible that the four carbonyl ligands co-ordinated to the iron atoms of the Fe–Fe edge not bridged by a phosphido group may scramble to give one resonance, with the other being due to the terminal carbonyl ligands on the remaining iron atom. It is noteworthy that even in the presence of an excess of phosphine or phosphite only one terminal carbonyl could be substituted.

III. Reaction of $[Fe_3(\mu_3\text{-}S)(\mu\text{-}PPh_2)_2(\mu\text{-}CO)(CO)_6]$ 1 with RC≡CH at elevated temperature and pressure

The reaction of $[Fe_3(\mu_3\text{-}S)(\mu\text{-}PPh_2)_2(\mu\text{-}CO)(CO)_6]$ **1** with RC≡CH [R = Ph or CH_2OH] in toluene at 423 K gives the complexes $[Fe_2(\mu\text{-}PPh_2CHCRS)(\mu\text{-}PPh_2CHCR)(CO)_4]$ [R = Ph **4a** or CH_2OH **4b**] and, in the case of R = Ph, $[Fe_2(\mu\text{-}PPh_2)(\mu\text{-}PPh_2CHCPhS)(CO)_5]$ **5** in combined good yield (see Scheme 3). All the complexes have been characterised by ^1H, ^{13}C, ^{31}P NMR and IR spectroscopy and by mass spectrometry and microanalysis (see Table 1 and Experimental section). In addition **4a** has been the subject of a single crystal X-ray diffraction study.

Table 3 Selected bond distances (Å) and angles (°) for complex $[Fe_3(\mu_3\text{-}S)(\mu\text{-}PPh_2)_2(\mu\text{-}CO)(CO)_5(PPhMe_2)]$ **3c**

Fe(1)–Fe(2)	2.503(2)	Fe(1)–Fe(3)	2.595(1)
Fe(2)–Fe(3)	2.531(1)	Fe(1)–S	2.244(2)
Fe(2)–S	2.237(2)	Fe(3)–S	2.265(2)
Fe(1)–P(1)	2.232(3)	Fe(2)–P(2)	2.171(2)
Fe(3)–P(2)	2.235(2)	Fe(1)–P(3)	2.232(2)
Fe(3)–P(3)	2.221(2)	Fe(1)–C(1)	1.863(9)
Fe(2)–C(1)	2.130(9)	P(1)–C(111)	1.825(8)
P(1)–C(121)	1.831(8)	P(1)–C(131)	1.828(8)
P(2)–C(211)	1.834(7)	P(2)–C(221)	1.837(8)
P(3)–C(311)	1.817(7)	P(3)–C(321)	1.822(7)
C(1)–O(1)	1.180(9)		
Fe–C (carbonyl)	1.750(9)–1.775(8)	C–O (carbonyl)	1.143(8)–1.162(9)
Fe(2)–Fe(1)–Fe(3)	59.50(4)	Fe(2)–Fe(1)–S	55.91(6)
Fe(2)–Fe(1)–P(1)	135.00(8)	Fe(2)–Fe(1)–P(3)	113.65(7)
Fe(2)–Fe(1)–C(1)	56.1(3)	Fe(3)–Fe(1)–S	55.23(6)
Fe(3)–Fe(1)–P(1)	141.85(8)	Fe(3)–Fe(1)–P(3)	54.15(6)
Fe(3)–Fe(1)–C(1)	115.0(3)	S–Fe(1)–C(1)	93.6(3)
P(1)–Fe(1)–S	100.28(9)	P(1)–Fe(1)–P(3)	99.69(9)
P(3)–Fe(1)–S	85.25(8)	P(3)–Fe(1)–C(1)	167.0(3)
Fe(1)–Fe(2)–Fe(3)	62.07(4)	Fe(1)–Fe(2)–S	56.18(6)
Fe(1)–Fe(2)–P(2)	117.97(7)	Fe(1)–Fe(2)–C(1)	46.6(2)
Fe(3)–Fe(2)–S	56.31(6)	Fe(3)–Fe(2)–P(2)	56.14(6)
Fe(3)–Fe(2)–C(1)	108.1(2)	S–Fe(2)–C(1)	86.9(3)
P(2)–Fe(2)–S	84.63(8)	P(2)–Fe(2)–C(1)	164.2(2)
Fe(1)–Fe(3)–Fe(2)	58.43(4)	Fe(1)–Fe(3)–S	54.48(6)
Fe(1)–Fe(3)–P(2)	111.98(7)	Fe(1)–Fe(3)–P(3)	54.56(6)
Fe(2)–Fe(3)–S	55.27(6)	Fe(2)–Fe(3)–P(2)	53.75(6)
Fe(2)–Fe(3)–P(3)	112.98(7)	P(2)–Fe(3)–P(2)	165.78(9)
Fe(1)–S–Fe(2)	67.91(7)	Fe(1)–S–Fe(3)	70.29(7)
Fe(2)–S–Fe(3)	68.42(7)	Fe(2)–P(2)–Fe(3)	70.11(7)
Fe(1)–P(3)–Fe(3)	71.29(7)	Fe(1)–C(1)–Fe(2)	77.3(3)

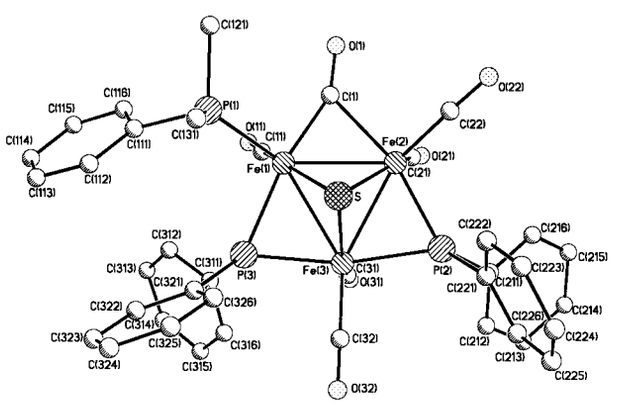

Fig. 3 Molecular structure of $[Fe_3(\mu_3\text{-}S)(\mu\text{-}PPh_2)_2(CO)_6(PPhMe_2)]$ **3c** including the atom numbering scheme. Hydrogen atoms have been omitted for clarity.

The complex $[Fe_2(\mu\text{-}PPh_2CHCPhS)(\mu\text{-}PPh_2CHCPh)(CO)_4]$ **4a** crystallizes with two molecules in the asymmetric unit. The molecules have opposing chirality but are otherwise virtually identical apart from a marked difference in the relative orientation of the phenyl rings C(241)–C(246) and C(211)–C(216) (see Fig. 4). Selected bond distances and angles are given in Table 4 with mean values used in the following discussion.

The structure of complex **4a** consists of an iron–iron vector bridged both by a seven-electron donating ligand [μ-PPh_2-CHCPhS] and by a three-electron donating ligand [μ-PPh_2-CH=CPh] and ligated terminally by carbonyl groups. The μ-$PPh_2CHCPhS$ ligand is incorporated into a five-membered metallacycle [Fe(2)–P(2)–C(3)=C(4)–S(1)] with the olefinic group π co-ordinated [Fe(1)–C(3) 2.150(9); Fe(1)–C(4) 2.08(2) Å] and the sulfur atom σ co-ordinated to the other iron centre

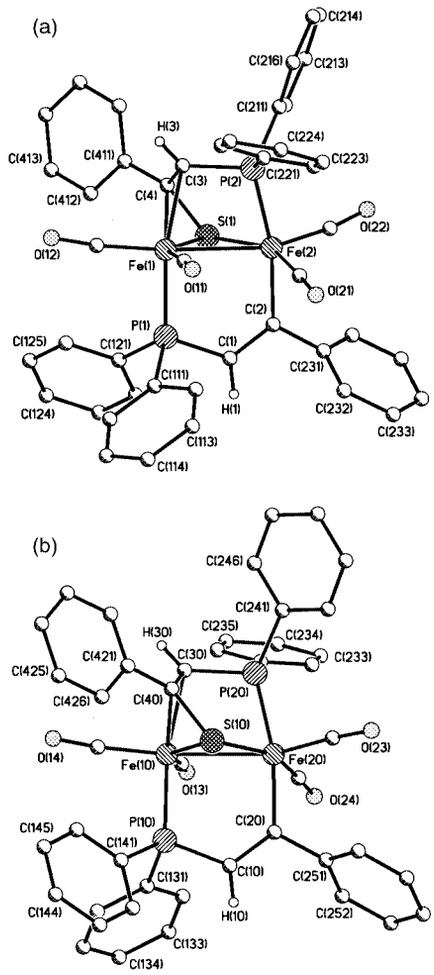

Fig. 4 The molecular structures and atom numbering schemes of the two independent enantiomers (a, molecule 1; b, molecule 2) of $[Fe_2(\mu\text{-}PPh_2CHCPhS)(\mu\text{-}PPh_2CHCPh)(CO)_4]$ **4a**. There is a very marked difference in rotation of the equivalent phenyl rings C(241)–C(246) and C(211)–C(216). Phenyl hydrogen atoms have been omitted for clarity.

[Fe(1)]. In contrast, the $\mu\text{-}PPh_2CH{=}CPh$ ligand forms part of a five-membered dimetallacycle [Fe(2)–C(2)=C(1)–P(1)–Fe(1)], in which the olefinic portion is not involved in co-ordination to either metal centre; the short C(1)–C(2) bond length of 1.374(9) Å is consistent with significant C=C character. The distorted octahedral co-ordination geometry at each iron atom is completed by carbonyl groups, two on each metal centre, of which one occupies a pseudo-axial and the other a pseudo-equatorial site (relative to the metal–metal bond). The metal–metal distance [Fe(1)–Fe(2) 2.703(2) Å] is consistent with the presence of a single Fe–Fe bond (as required by the EAN rule) although it is in the upper range for related metallacyclic-bridged diiron complexes.[5,17]

While examples of bimetallic complexes bridged by PPh_2-CRCR ligands in which the ligand is incorporated into a metallaphosphabutene ring have been well documented,[9,18] structurally characterised examples in which PPh_2CRCR forms part of a dimetallaphosphapentene ring as in **4a** are rare.[7] Furthermore, the cycloferraphosphathiapentene system formed by the $\mu\text{-}PPh_2CHCPhS$ ligand appears, to the knowledge of the authors, unprecedented.

The spectroscopic properties of complex **4a** are in accordance with the solid state structure being maintained in solution. In the $^{31}P\text{-}\{^1H\}$ NMR spectrum two doublet resonances are seen with chemical shifts [δ −66.2 and −68.2] typical of a diphenylphosphide fragment contained within a metallacycle[7,17c] and a coupling constant [^3J(PP) 18.3 Hz] characteristic of a phosphorus atom coupling to another phosphorus through three bonds. The $^{13}C\text{-}\{^1H\}$ NMR spectrum at ambient temperature shows, in addition to signals corresponding to phenyl carbon atoms, four signals at lower field [δ 221.5, 219.9, 214.9, 210.6] due to four inequivalent terminal carbonyl ligands. By comparison with the spectroscopically characterised complex $[Fe_2(\mu\text{-}SPh)\{\mu\text{-}PPh_2CHC(CH_2OH)\}(CO)_6]$[7] the resonance corresponding to the α-carbon of the non-π-co-ordinating ligand $\mu\text{-}PPh_2C_\beta HC_\alpha Ph$ can clearly be identified as a doublet of doublets, ^2J(PC) 35, 35 Hz, at δ 203.6 while the β-carbon atom resonance is masked by that due to the phenyl carbon atoms. On the other hand the α-carbon of the π-co-ordinated $\mu\text{-}PPh_2C_\beta HC_\alpha PhS$ ligand is seen as a doublet, ^2J(PC) 27 Hz, at δ 157.0 and the β-carbon as a doublet of doublets, ^1J(PC) 41, ^3J(PC) 7 Hz, at δ 47.6; these coupling constants are comparable with those found for structurally related $\mu\text{-}PPh_2CHCPhC(O)$ dicobalt complexes.[19] In the ^1H NMR spectrum of **4a** two resonances integrating as one proton each are seen for the two CH protons within the complex. The more downfield doublet of doublet resonance, ^2J(PH) 20.4, ^4J(PH) 5.8 Hz, at δ 6.39 is assigned to the $PPh_2C\mathit{H}CPh$ proton while the singlet at δ 4.08 is assigned to the $PPh_2C\mathit{H}CPhS$ proton. Complex **4b** is assigned an analogous structure to that of **4a** on the basis of spectroscopic data (see Table 1 and Experimental section).

The structure of $[Fe_2(\mu\text{-}PPh_2)(\mu\text{-}PPh_2CHCPhS)(CO)_5]$ **5** has been assigned on the basis of spectroscopic data. The FAB mass spectrum displays a molecular ion peak consistent with the above formulation and fragmentation peaks corresponding to the loss of up to five carbonyl groups. In the $^{31}P\text{-}\{^1H\}$ NMR spectrum two doublet resonances are observed, the downfield resonance [δ −1.5, ^2J(PP) 78.0] being assigned to a phosphido group bridging two iron atoms[5,10b] while the upfield resonance [δ −54.2, ^2J(PP) 78.0 Hz] is comparable with the chemical shift for the phosphorus atom in the $PPh_2CHCPhS$ ligand in **4a** [δ *ca.* −66.0]. The ^1H NMR spectrum of complex **5** shows resonances corresponding to phenyl protons and a doublet resonance assignable to the olefinic proton at δ 6.88 [^2J(PH) 6.8 Hz, $\mu\text{-}PPh_2C\mathit{H}CPhS$], the downfield positioning of this signal suggesting the vinyl group of the $\mu\text{-}PPh_2CHCPhS$ ligand is not π co-ordinated to an iron atom. The possible formulation of the complex as $[Fe_2(\mu\text{-}SPPh_2)(\mu\text{-}PPh_2CHCPh)(CO)_5]$ is rejected due to comparison of the spectroscopic data with those of known complexes containing $\mu\text{-}PPh_2S$ ligands.[6,20]

The degradation of the sulfur-capped trinuclear clusters on reaction with alkynes is unusual.[4a] Scheme 4 shows a possible pathway that could account for the formation of complexes **4** and **5**. Initial insertion of an alkyne group into the metal–phosphorus bond in **1** may yield an intermediate complex $[Fe_3(\mu_3\text{-}S)(\mu\text{-}PPh_2)(\mu\text{-}PPh_2CH{=}CR)(\mu\text{-}CO)(CO)_6]$ **A**, with a subsequent internal rearrangement resulting in the formation of the intermediate complex $[Fe_3(\mu\text{-}PPh_2)(\mu\text{-}PPh_2CH{=}CRS)(CO)_8]$ **B**. The rearrangement of the bridging phosphido group and cleavage of the two iron–iron bonds may then give **5**, with further insertion of an alkyne molecule to give **4**. On standing, complex **5** readily undergoes a partial decomposition process, in which phenylacetylene is liberated and thus able to recombine with intact molecules of **5** to generate **4a**; this suggests that **5** is a precursor to **4a**.

It is noteworthy that we have previously observed that treatment of the related complex $[Co_3(\mu_3\text{-}S)(\mu\text{-}PPh_2)(CO)_6(PPh_3)]$ with PhC≡CH results in preservation of the tricobalt core and insertion into a metal–phosphorus bond to give $[Co_3(\mu_3\text{-}S)(\mu\text{-}PPh_2CHCPh)(CO)_6(PPh_3)]$, a transformation that is consistent with the first step of the proposed reaction pathway. Furthermore, the reaction of $[Fe_2(\mu\text{-}PPh_2)(\mu\text{-}SPh)(CO)_6]$ with $(HOCH_2)C{\equiv}CH$ has been demonstrated to give the related $PPh_2CHC(CH_2OH)$-bridged product $[Fe_2(\mu\text{-}SPh)\{\mu\text{-}PPh_2CHC(CH_2OH)\}(CO)_6]$, a step that is related to the iron–phosphorus bond insertion reaction proposed in the conversion of **5** into **4**.[7]

Table 4 Selected bond distances (Å) and angles (°) for complex $[Fe_2(\mu\text{-}PPh_2CHCPhS)(\mu\text{-}PPh_2CHCPh)(CO)_4]$ **4a**

	Molecule 1	Molecule 2		Molecule 1	Molecule 2
Fe(1)–Fe(2)	2.704(2)	2.702(2)	Fe(1)–P(1)	2.236(4)	2.231(4)
Fe(1) · · · P(2)	3.021(5)	3.023(5)	Fe(1)–S(1)	2.226(4)	2.240(4)
Fe(1)–C(3)	2.149(9)	2.151(9)	Fe(1)–C(4)	2.07(2)	2.10(2)
Fe(2)–P(2)	2.218(4)	2.227(4)	Fe(2)–S(1)	2.199(3)	2.193(4)
Fe(2)–C(2)	2.028(7)	2.029(7)	P(1)–C(1)	1.80(1)	1.79(2)
P(2)–C(3)	1.82(1)	1.80(1)	S(1)–C(4)	1.74(2)	1.77(2)
C(1)–C(2)	1.368(9)	1.380(9)	C(3)–C(4)	1.399(9)	1.393(9)
P–C (phenyl)	1.80(1)–1.84(1)	1.81(1)–1.85(1)			
Fe–C (carbonyl)	1.745(8)–1.757(8)	1.735(8)–1.763(9)			
C–O (carbonyl)	1.14(2)–1.20(2)	1.14(1)–1.18(2)			
Fe(2)–Fe(1)–P(1)	88.9(2)	89.3(2)	Fe(2)–Fe(1)–S(1)	51.9(1)	51.7(1)
Fe(2)–Fe(1)–C(3)	77.6(4)	78.3(4)	Fe(2)–Fe(1)–C(4)	81.5(4)	81.3(4)
P(1)–Fe(1)–S(1)	87.0(2)	87.6(2)	P(1)–Fe(1)–C(3)	161.9(4)	163.0(4)
P(1)–Fe(1)–C(4)	127.9(4)	128.9(4)	P(2)–Fe(1)–C(3)	36.4(3)	36.1(3)
S(1)–Fe(1)–C(3)	75.3(4)	75.7(4)	S(1)–Fe(1)–C(4)	47.7(4)	48.1(4)
C(3)–Fe(1)–C(4)	38.7(3)	38.3(3)	C(4)–Fe(1)–P(2)	62.0(3)	60.0(3)
Fe(1)–Fe(2)–P(2)	75.0(2)	75.0(1)	Fe(1)–Fe(2)–S(1)	52.8(1)	53.2(1)
Fe(1)–Fe(2)–C(2)	93.2(3)	93.3(3)	P(2)–Fe(2)–S(1)	88.8(2)	87.4(2)
P(2)–Fe(2)–C(2)	168.0(4)	168.0(4)	S(1)–Fe(2)–C(2)	86.0(4)	87.7(4)
Fe(1)–P(1)–C(1)	110.7(5)	110.5(5)	Fe(1)–P(2)–Fe(2)	59.8(1)	59.7(1)
Fe(1)–P(2)–C(3)	44.7(3)	44.6(3)	Fe(2)–P(2)–C(3)	98.7(4)	99.7(4)
Fe(1)–S(1)–Fe(2)	75.1(1)	75.1(1)	Fe(1)–S(1)–C(4)	61.3(6)	61.7(6)
Fe(2)–S(1)–C(4)	105.6(4)	105.2(4)	P(1)–C(1)–C(2)	123(1)	124(1)
Fe(2)–C(2)–C(1)	124(1)	123(1)	Fe(1)–C(3)–P(2)	98.9(5)	99.4(5)
Fe(1)–C(3)–C(4)	67.4(8)	68.7(9)	P(2)–C(3)–C(4)	116(1)	114(1)
Fe(1)–C(4)–S(1)	71.0(7)	70.3(7)	Fe(1)–C(4)–C(3)	73.9(8)	73.0(8)
S(1)–C(4)–C(3)	116(1)	116(1)			

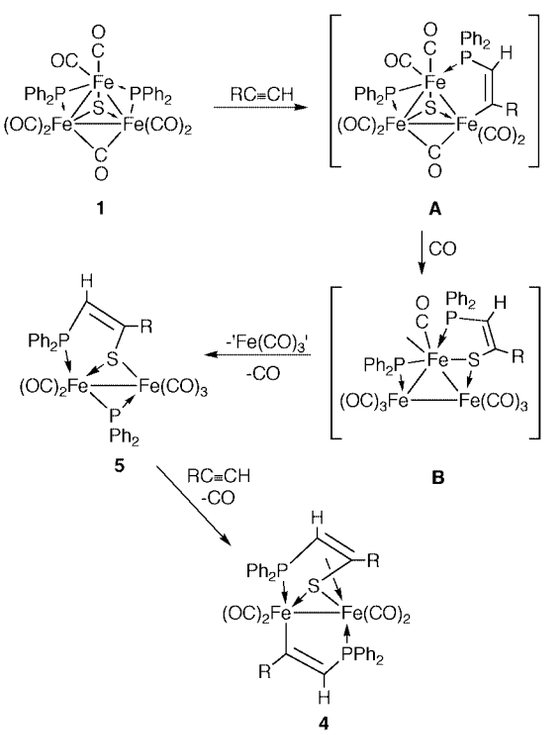

Scheme 4 Possible pathway to account for the formation of complexes **4** and **5** (R = Ph or CH_2OH).

Conclusion

The use of $Ph_2P(SCMe_3)$ in place of $Ph_2P(SPh)$ in the reaction with $[Fe(CO)_5]$ results in sulfur–carbon bond cleavage and yields as the major product the triiron cluster $[Fe_3(\mu_3\text{-}S)(\mu\text{-}PPh_2)(\mu\text{-}CO)(CO)_6]$ **1**. The outcome of reaction of **1** with a range of ligands has been examined and found to depend on the ligand employed. With organo-phosphites and -phosphines the trinuclear framework is maintained and substitution of a terminal carbonyl group occurs to give **3**. In contrast treatment of **1** with alkynes results in breakdown of the $Fe_3(\mu_3\text{-}S)$ core to give the bimetallic complexes **4** and **5** in which new sulfur–carbon and phosphorus–carbon bonds have formed.

Experimental

General techniques

All reactions were carried out under a nitrogen atmosphere using standard Schlenk techniques. Solvents were distilled under nitrogen from appropriate drying agents and degassed prior to use. Preparative thin-layer chromatography (TLC) was carried out on commercial Merck plates with a 0.25 mm layer of silica, or on 1 mm silica plates prepared at the University Chemical Laboratory, Cambridge. Column chromatography was performed on Kieselgel 60 (70–230 or 230–400 mesh). Products are given in order of decreasing R_f values.

The instrumentation used to obtain spectroscopic data has been described previously.[21] Unless otherwise stated all reagents were obtained from commercial suppliers; $Ph_2P(SCMe_3)$ was prepared by the literature method.[11]

Syntheses of complexes

$[Fe_3(\mu_3\text{-}S)(\mu\text{-}PPh_2)_2(\mu\text{-}CO)(CO)_6]$ 1 and $[\{Fe_2(\mu\text{-}PPh_2)(CO)_6\}_2(\mu_4\text{-}S_2)]$ 2. A solution of $[Fe(CO)_5]$ (1.0 ml, 7.60 mmol) and $Ph_2P(SCMe_3)$ (2.00 g, 7.28 mmol) in toluene (50 ml) was added to a 100 ml Roth autoclave and pressurised with 5 atm of CO. The sealed system was stirred at 423 K for 20 h. After removal of the solvent under reduced pressure, the mixture was purified using preparative TLC with hexane–dichloromethane (10 : 1) as eluent. This gave in addition to decomposition products the orange crystalline $[\{Fe_2(\mu\text{-}PPh_2)(CO)_6\}_2(\mu\text{-}S_2)]$ **2** (0.099 g, 3%) and green crystalline $[Fe_3(\mu_3\text{-}S)(\mu\text{-}PPh_2)_2(\mu\text{-}CO)(CO)_6]$ **1** (0.576 g, 31%) complexes. Calc. for $C_{31}H_{20}Fe_3O_7P_2S$ (**1**): C, 48.5; H, 2.6. Found: C, 48.1; H, 2.5%. Fast atom bombardment (FAB) mass spectrum: *m/z* 766 (M^+) and

Table 5 X-Ray crystallographic and data processing parameters for complexes **2**, **3c** and **4a**

	2	**3c**	**4a**
Empirical formula	$C_{36}H_{20}Fe_4O_{12}P_2S_2$	$C_{38}H_{31}Fe_3O_6P_3S$	$C_{44}H_{32}Fe_2O_4P_2S$
Formula weight	993.68	876.15	830.40
T/K	293(2)	293(2)	293(2)
Crystal system	Triclinic	Orthorhombic	Monoclinic
Space group	$P\bar{1}$ (no. 2)	$P2_12_12_1$	$P2_1$
a/Å	10.271(2)	12.574(2)	11.103(3)
b/Å	10.675(2)	16.1199(13)	35.620(4)
c/Å	11.517(2)	18.8859(15)	10.898(3)
α/°	102.19(3)	—	—
β/°	102.93(3)	—	117.62(2)
γ/°	117.93(3)	—	—
U/Å^3	1011.6(4)	3827.9(8)	3818.8(7)
Z	1	4	4
μ(Mo-Kα)/mm^{-1}	1.647	1.346	0.940
Reflections collected	5778	4699	5787
Independent reflections	5024 [R(int) = 0.0207]	4476 [R(int) = 0.0330]	3117 [$I > 3\sigma(I)$]
Final $R1$, $wR2$			
$I > 2\sigma(I)$	0.0449, 0.0845	0.0473, 0.0760	0.0655, 0.0651[a]
All data	0.0812, 0.0986	0.0818, 0.0893	—

[a] R and R'.

$M^+ - n$CO(n = 1–7). NMR ($CDCl_3$): ^{13}C (^{1}H composite pulse decoupled), δ 214.6[dd, ^2J(PC) 16, 16, CO], 208.8[dd, ^2J(PC) 12, 12 Hz, CO] and 143–128[m, Ph]. Unit cell dimensions: a = 22.747(7), b = 8.8344(11), c = 34.485(8) Å, β = 93.46(2)°. FAB mass spectrum (**2**): m/z 497 (M^+) and $M^+ - n$CO(n = 1–6). NMR ($CDCl_3$): ^{13}C (^{1}H composite pulse decoupled), δ 135–128[m, Ph].

[$Fe_3(\mu_3$-S)(μ-$PPh_2)_2(\mu$-CO)(CO)$_5$(L)] [L = P(OMe)$_3$ 3a, P(OPh)$_3$ 3b, $PPhMe_2$ 3c or PPh_3 3d]. To solutions of [$Fe_3(\mu_3$-S)(μ-$PPh_2)_2(\mu$-CO)(CO)$_6$] **1** (0.200 g, 0.27 mmol) in toluene (50 ml) an excess of phosphite/phosphine (L) [L = P(OMe)$_3$, 0.2 ml, 1.70 mmol; P(OPh)$_3$, 0.2 ml, 1.15 mmol; $PPhMe_2$, 0.2 ml, 1.40 mmol; PPh_3, 0.200 g, 0.76 mmol] was added. These solutions were stirred at 373 K for 6 h and after removal of the solvents under reduced pressure the mixture was absorbed onto the minimum amount of silica, added to the top of a chromatography column and purified with hexane–dichloromethane (10:1) [L = $PPhMe_2$ or PPh_3] or hexane–dichloromethane (2:1) [L = P(OMe)$_3$ or P(OPh)$_3$] as eluent. This gave in addition to unchanged starting material the green crystalline complexes [$Fe_3(\mu_3$-S)(μ-$PPh_2)_2(\mu$-CO)(CO)$_5$-(L)] [L = P(OMe)$_3$ (0.146 g, 65%) **3a**; P(OPh)$_3$ (0.137 g, 57%) **3b**; $PPhMe_2$ (0.139 g, 61%) **3c**; or PPh_3 (0.115 g, 44%) **3d**. FAB mass spectrum (**3a**): m/z 862 (M^+) and $M^+ - n$CO(n = 1–6). NMR ($CDCl_3$): ^{13}C (^{1}H composite pulse decoupled), δ 215.9[s, br, CO], 209.8[s, br, CO], 145–127[m, Ph] and 55.6[d, ^2J(PC) 6 Hz, P(OMe)$_3$]. Calc. for $C_{48}H_{35}Fe_3O_9P_3S$ (**3b**): C, 54.9; H, 3.3. Found: C, 54.4; H, 3.4%. FAB mass spectrum: m/z 1049 (M^+) and $M^+ - n$CO(n = 1–6). NMR ($CDCl_3$): ^{13}C (^{1}H composite pulse decoupled), δ 215.7[dd, ^2J(PC) 16, 15, CO], 209.3[dd, ^2J(PC) 11, 11 Hz, CO] and 151–121[m, Ph]. Calc. for $C_{38}H_{31}Fe_3O_6P_3S$ (**3c**): C, 52.1; H, 3.5. Found: C, 52.1; H, 3.6%. FAB mass spectrum: m/z 876 (M^+) and $M^+ - n$CO(n = 1–6). NMR ($CDCl_3$): ^{13}C (^{1}H composite pulse decoupled), δ 216.0 [s, br, CO], 209.8[s, br, CO], 145–127[m, Ph] and 19.2[d, ^1J(PC) 28 Hz, $PPhMe_2$]. Calc. for $C_{48}H_{35}Fe_3O_6P_3S$ (**3d**): C, 57.5; H, 3.5. Found: C, 57.6; H, 3.8%. FAB mass spectrum: m/z 1001 (M^+) and $M^+ - n$CO(n = 1–6). NMR ($CDCl_3$): ^{13}C (^{1}H composite pulse decoupled), δ 216.5[dd, ^2J(PC) 15, 15, CO], 209.6[dd, ^2J(PC) 9, 9 Hz, CO] and 144–128[m, Ph].

[$Fe_2(\mu$-PPh_2CHCRS)(μ-PPh_2CH=CR)(CO)$_4$] [R = Ph 4a or CH_2OH 4b] and [$Fe_2(\mu$-$PPh_2)$(μ-PPh_2CHCPhS)(CO)$_5$] 5. A solution of [$Fe_3(\mu_3$-S)(μ-$PPh_2)_2(\mu$-CO)(CO)$_6$] **1** (0.200 g, 0.27 mmol) and RC≡CH [R = Ph (0.2 ml, 1.82 mmol) or CH_2OH (0.2 ml, 3.44 mmol)] in toluene (50 ml) was added to a 100 ml Roth autoclave and pressurised with 5 atm of CO. The sealed system was stirred at 423 K for 20 h. After removal of the solvent under reduced pressure the mixture was purified using preparative TLC with hexane–dichloromethane (10:1) [R = Ph] or hexane–ethyl acetate (5:1) [R = CH_2OH] as eluent. This gave, in addition to decomposition products, orange crystalline [$Fe_2(\mu$-PPh_2CHCRS)(μ-PPh_2CH=CR)(CO)$_4$] [R = Ph (0.151 g, 45%) **4a** or CH_2OH (0.123 g, 41%) **4b**] and [$Fe_2(\mu$-$PPh_2)$-(μ-PPh_2CHCPhS)(CO)$_5$] **5** (0.43 g, 14%). Calc. for $C_{44}H_{32}$-$Fe_2O_4P_2S$ (**4a**): C, 63.6; H, 3.9. Found: C, 63.8; H, 4.1%. FAB mass spectrum: m/z 830 (M^+) and $M^+ - n$CO(n = 1–4). NMR ($CDCl_3$): ^{13}C (^{1}H composite pulse decoupled), δ 221.5[dd, ^2J(PC) 11, 7, CO], 219.9[d, ^2J(PC) 15, CO], 214.9[d, ^2J(PC) 16, CO], 210.6[d, ^2J(PC) 22, CO], 203.6[dd, ^2J(PC) 35, 35, PPh_2-CH*C*Ph], 157.0[d, ^2J(PC) 27, PPh_2CH*C*PhS], 137–120[m, Ph, PPh_2*C*HCPh] and 47.6[dd, ^1J(PC) 41, ^3J(PC) 7 Hz, PPh_2-*C*HCPhS]. FAB mass spectrum (**4b**): m/z 738 (M^+) and $M^+ - n$CO(n = 1–4). NMR ($CDCl_3$): ^{13}C (^{1}H composite pulse decoupled), δ 220.7[d, ^2J(PC) 12, CO], 218.9[d, ^2J(PC) 15, CO], 215.5[d, ^2J(PC) 16, CO], 210.6[d, ^2J(PC) 19, CO], 203.6[dd, ^2J(PC) 35, 35, PPh_2CH*C*(CH_2OH)], 140.3[d, ^2J(PC) 22, PPh_2-CH*C*(CH_2OH)S], 135–125[m, Ph, PPh_2*C*HC(CH_2OH)], 74.3[d, ^2J(PC) 26, PPh_2CHC(*C*H_2OH)], 68.1[s, PPh_2CHC(*C*H_2OH)S] and 47.6[dd, ^1J(PC) 41, ^3J(PC) 7 Hz, PPh_2*C*HC(CH_2OH)S]. FAB mass spectrum (**5**): m/z 756 (M^+) and $M^+ - n$CO(n = 1–5).

Crystal structure determinations of complexes 2, 3c and 4a

For complexes **2** and **3c** X-ray intensity data were collected on a Siemens P4 four-circle diffractometer and for **4a** on a Phillips PW1100 four-circle diffractometer. Table 5 lists details of data collection, refinement and crystal data. Data were corrected for Lorentz and polarisation factors.

For all structures the metal positions were deduced from the Patterson method and subsequent Fourier-difference syntheses revealed the positions of the remaining non-hydrogen atoms. For **2** and **3c**, refinements were performed using SHELXTL[22] based on F^2 and for **4a** with SHELX 76 based on F.[23] The phenyl rings in **3c** and **4a** were constrained to refine as rigid hexagons. The phenyl ring hydrogen atoms were placed in calculated positions with displacement parameters equal to 1.2U_{eq} of the parent carbon atoms for **2** and **3c**, and those of **4a** were fixed at 0.08 Å^2. There were two independent molecules per equivalent position in the crystal structure of **4a**. After initial refinement with isotropic displacement parameters,

empirical absorption corrections were applied to the data of **2**, **3c** and **4a**.[24] Anisotropic displacement parameters were assigned in structures **2** and **3c** to all non-hydrogen atoms and in **4a** to only the iron, phosphorus, sulfur and carbonyl atoms.

The correct stereochemistry of the refined molecule depicted in Fig. 3 is confirmed by the Flack parameter of −0.01(3). Clearly, as complex **3c** is racemic, equal numbers of both enantiomers will be present in the bulk sample. The racemic mixture of **4a** also crystallises in a chiral space group ($P2_1$) but in this case both enantiomers are present in the same crystal; molecules of opposing stereochemistry are paired in a chiral arrangement in the asymmetric unit. Equivalent bond lengths in the two molecules were constrained to be equal within an e.s.d. of 0.05 (Fe–Fe) or 0.01 Å (bonds involving other atoms). Inverting the chirality of the molecules made negligible difference to *R*.

CCDC reference number 186/1673.

See http://www.rsc.org/suppdata/dt/1999/3941/ for crystallographic files in .cif format.

Acknowledgements

This work was supported by the EPSRC (grants to G. E. P. and G. A. S.).

References

1 M. G. Kanatzidis and S.-P. Huang, *J. Coord. Chem. Rev.*, 1994, **130**, 509; A. Muller, *Polyhedron*, 1986, **5**, 323; L. C. Roof and J. W. Kolis, *Chem. Rev.*, 1993, **93**, 1037.

2 P. E. Eldredge and B. A. Averill, *J. Cluster Sci.*, 1990, **1**, 269; P. Zanello, *Coord. Chem. Rev.*, 1988, **83**, 199; **87**, 1; D. C. Rees, M. K. Chan and J. Kim, *Adv. Inorg. Chem.*, 1994, **40**, 89; D. Coucouvanis, in *Molybdenum Enzymes, Cofactors and Model Systems*, eds. E. I. Stiefel, D. Coucouvanis and W. E. Newton, American Chemical Society, Washington, DC, 1993, p. 304.

3 R. J. Angelici, *Acc. Chem. Res.*, 1988, **21**, 387; B. C. Wiegand and C. M. Friend, *Chem. Rev.*, 1992, **92**, 491; C. Bianchini and A. Meli, *J. Chem. Soc.*, *Dalton Trans.*, 1996, 801; V. Riaz, O. J. Curnow and M. D. Curtis, *J. Am. Chem. Soc.*, 1994, **116**, 4357.

4 (*a*) K. Hashizume, Y. Mizobe and M. Hidai, *Organometallics*, 1995, **14**, 5367; (*b*) E. Roland and H. Vahrenkamp, *J. Mol. Catal.*, 1983, **21**, 233; (*c*) W. Bernhardt, C. von Schnering and H. Vahrenkamp, *Angew. Chem.*, *Int. Ed. Engl.*, 1986, **25**, 279.

5 A. J. Carty, *Adv. Chem. Ser.*, 1982, **196**, 163; *Pure Appl. Chem.*, 1982, **54**, 113.

6 See A. Martín, M. J. Mays, P. R. Raithby and G. A. Solan, *J. Chem. Soc.*, *Dalton Trans.*, 1993, 1789 and refs. therein.

7 A. J. Edwards, A. Martín, M. J. Mays, D. Nazar, P. R. Raithby and G. A. Solan, *J. Chem. Soc.*, *Dalton Trans.*, 1993, 355.

8 A. J. Edwards, A. Martín, M. J. Mays, P. R. Raithby and G. A. Solan, *J. Chem. Soc.*, *Chem. Commun.*, 1992, 1416.

9 A. Martín, M. J. Mays, P. R. Raithby and G. A. Solan, *J. Chem. Soc.*, *Dalton Trans.*, 1993, 1431; S. L. Ingham, M. J. Mays, P. R. Raithby, G. A. Solan, B. V. Sundavadra, G. Conole and M. Kessler, *J. Chem. Soc.*, *Dalton Trans.*, 1994, 3607.

10 (*a*) B. E. Job, R. A. N. Mclean and D. T. Thompson, *Chem. Commun.*, 1966, 895; (*b*) G. L. Borgne and R. Mathieu, *J. Organomet. Chem.*, 1981, **208**, 201.

11 G. Conole, M. Kessler, M. J. Mays, G. E. Pateman and G. A. Solan, *Polyhedron*, 1998, **17**, 2993.

12 For other examples of complexes with a $Fe_3(\mu_3\text{-S})$ core see: L. Markó, T. Madach and H. Vahrenkamp, *J. Organomet. Chem.*, 1980, **190**, C67; G. Hogarth, N. J. Taylor, A. J. Carty and A. Meyer, *J. Chem. Soc.*, *Chem. Commun.*, 1988, 834; F. T. Al-Ani, D. L. Hughes and C. J. Pickett, *J. Organomet. Chem.*, 1986, **307**, C31; F. Caleroni, F. Demartin, M. C. Iapalucci, F. Laschi, G. Longoni and P. Zanello, *Inorg. Chem.*, 1996, **35**, 898.

13 D. E. Barber, M. Sabat, E. Sinn and B. A. Averill, *Organometallics*, 1995, **14**, 3229; S. Inomata, H. Takano, K. Hiyama, H. Tobita and H. Ogino, *Organometallics*, 1995, **14**, 2112.

14 K. S. Bose, E. Sinn and B. A. Averill, *Organometallics*, 1984, **3**, 1126.

15 See for example, Ch. Elschenbroich and A. Salzer, *Organometallics*, B. G. Tauber, Stuttgart, 1988, ch. 13 and refs. therein.

16 K. Hashizume, Y. Mizobe and M. Hidai, *Organometallics*, 1996, **15**, 3303; Z. Tang, Y. Nomura, Y. Ishii, Y. Mizobe and M. Hidai, *Organometallics*, 1997, **16**, 151.

17 (*a*) See for example, R. Rumin, K. Guennou, F. Y. Pétillon and K. W. Muir, *J. Chem. Soc.*, *Dalton Trans.*, 1997, 1381 and refs. therein; (*b*) W. F. Smith, N. J. Taylor and A. J. Carty, *J. Chem. Soc.*, *Chem. Commun.*, 1976, 896; (*c*) M. Etienne, R. Mathieu and N. Lugan, *Organometallics*, 1993, **12**, 140.

18 H. Yamazaki, K. Aoki and H. Yamazaki, *J. Organomet. Chem.*, 1975, **84**, C28; B. L. Barnett and C. Kruger, *Cryst. Struct. Commun.*, 1973, **2**, 347; R. Regragui, P. H. Dixneuf, N. J. Taylor and A. J. Carty, *Organometallics*, 1984, **3**, 814; 1990, **9**, 2234; H. Werner and R. Zolk, *Chem. Ber.*, 1987, **120**, 1003; B. Klingert, A. L. Rheingold and H. Werner, *Inorg. Chem.*, 1988, **27**, 1354; G. Conole, K. A. Hill, M. McPartlin, M. J. Mays and M. J. Morris, *J. Chem. Soc.*, *Chem. Commun.*, 1989, 688.

19 A. J. M. Caffyn, M. J. Mays, G. A. Solan, D. Braga, P. Sabatino, G. Conole, M. McPartlin and H. R. Powell, *J. Chem. Soc.*, *Dalton Trans.*, 1991, 3103.

20 B. Messbauer, H. Meyer, B. Walther, M. J. Heeg, A. F. M. Maqsudar Rahman and J. P. Oliver, *Inorg. Chem.*, 1983, **22**, 272; K. P. Wagner, R. W. Hess, P. M. Treichel and J. C. Calabrese, *Inorg. Chem.*, 1975, **14**, 1121.

21 A. J. M. Caffyn, M. J. Mays and P. R. Raithby, *J. Chem. Soc.*, *Dalton Trans.*, 1991, 2349.

22 SHELXTL (PC version 5.03), Siemens Analytical Instruments Inc., Madison, WI, 1994.

23 G. M. Sheldrick, SHELX 76, program for crystal structure determination, University of Cambridge, 1976.

24 N. Walker and D. Stuart, *Acta Crystallogr.*, *Sect. A*, 1983, **39**, 158.

Paper 9/05931H